Diabetologia (2017) 60:1761–1769
DOI 10.1007/s00125-017-4327-y

ARTICLE

Diverse metabolic effects of *O*-GlcNAcylation in the pancreas but limited effects in insulin-sensitive organs in mice

Shogo Ida[1] · Katsutaro Morino[1] · Osamu Sekine[1] · Natsuko Ohashi[1] · Shinji Kume[1] · Tokuhiro Chano[2] · Kanako Iwasaki[3] · Norio Harada[3] · Nobuya Inagaki[3] · Satoshi Ugi[1] · Hiroshi Maegawa[1]

Received: 24 December 2016 / Accepted: 18 April 2017 / Published online: 22 June 2017

Abstract

Aims/hypothesis *O*-GlcNAcylation is characterised by the addition of *N*-acetylglucosamine to various proteins by *O*-GlcNAc transferase (OGT) and serves in sensing intracellular nutrients by modulating various cellular processes. Although it has been speculated that *O*-GlcNAcylation is associated with glucose metabolism, its exact role in whole body glucose metabolism has not been fully elucidated. Here, we investigated whether loss of *O*-GlcNAcylation globally and in specific organs affected glucose metabolism in mammals under physiological conditions.

Methods Tamoxifen-inducible global *Ogt*-knockout (*Ogt*-KO) mice were generated by crossbreeding *Ogt*-flox mice with *R26*-Cre-ER^{T2} mice. Liver, skeletal muscle, adipose tissue and pancreatic beta cell-specific *Ogt*-KO mice were generated by crossbreeding *Ogt*-flox mice with *Alb*-Cre, *Mlc1f*-Cre, *Adipoq*-Cre and *Pdx1*^{PB}-CreER™ mice, respectively. Glucose metabolism was evaluated by i.p. glucose and insulin tolerance tests.

Results Tamoxifen-inducible global *Ogt*-KO mice exhibited a lethal phenotype from 4 weeks post injection, suggesting that *O*-GlcNAcylation is essential for survival in adult mice. Tissue-specific *Ogt* deletion from insulin-sensitive organs, including liver, skeletal muscle and adipose tissue, had little impact on glucose metabolism under physiological conditions. However, pancreatic beta cell-specific *Ogt*-KO mice displayed transient hypoglycaemia (*Ogt*-flox 5.46 ± 0.41 vs *Ogt*-βKO 3.88 ± 0.26 mmol/l) associated with about twofold higher insulin secretion and accelerated adiposity, followed by subsequent hyperglycaemia (*Ogt*-flox 6.34 ± 0.32 vs *Ogt*-βKO 26.4 ± 2.37 mmol/l) with insulin depletion accompanied by beta cell apoptosis.

Conclusions/interpretation These findings suggest that *O*-GlcNAcylation has little effect on glucose metabolism in insulin-sensitive tissues but plays a crucial role in pancreatic beta cell function and survival under physiological conditions. Our results provide novel insight into *O*-GlcNAc biology and physiology in glucose metabolism.

Keywords Apoptosis · Beta cells · Insulin resistance · Insulin secretion · *O*-GlcNAc transferase · *O*-GlcNAcylation · Post-translational modification

Abbreviations

KO	Knockout
O-GlcNAc	O-linked *N*-acetylglucosamine
OGT	*O*-GlcNAc transferase
Ogt-βKO	Beta cell-specific *Ogt*-knockout mice
Ogt-FKO	Adipose tissue-specific *Ogt*-knockout mice
Ogt-LKO	Liver-specific *Ogt*-knockout mice
Ogt-MKO	Skeletal muscle-specific *Ogt*-knockout miceTM Tamoxifen
UDP-GlcNAc	Uridine diphosphate *N*-acetylglucosamine

Electronic supplementary material The online version of this article (doi:10.1007/s00125-017-4327-y) contains peer-reviewed but unedited supplementary material, which is available to authorised users.

✉ Katsutaro Morino
morino@belle.shiga-med.ac.jp

[1] Department of Medicine, Shiga University of Medical Science, Tsukinowa-cho, Seta, Otsu, Shiga 520-2192, Japan

[2] Department of Clinical Laboratory Medicine, Shiga University of Medical Science, Otsu, Shiga, Japan

[3] Department of Diabetes, Endocrinology and Nutrition, Graduate School of Medicine, Kyoto University, Kyoto, Japan

Introduction

Post-translational modifications to intracellular proteins regulate a variety of physiological cellular functions. Growing evidence indicates that dysfunction of post-translational modifications, including phosphorylation, ubiquitination and acetylation, disrupts cellular homeostasis and is strongly associated with the pathogenesis of numerous diseases, including metabolic disorders [1–3]. Thus, elucidation of the relationship between post-translational modifications and cellular physiology may be a first step to better understand disease pathogenesis and provide insight into the development of novel therapeutics.

O-GlcNAcylation has been analysed as an important regulator of glucose metabolism [4–6]. In a branch of the glycolytic pathway, fructose-6-phosphate is converted into uridine diphosphate *N*-acetylglucosamine (UDP-GlcNAc) through multiple enzymes in the hexosamine biosynthetic pathway. In this process, not only glucose but also glutamine and acetyl-CoA are integrated to form UDP-GlcNAc. *O*-GlcNAc transferase (OGT) is essential for *O*-GlcNAcylation and attaches *O*-GlcNAc to proteins at specific serine or threonine residues [7]. Thus, *O*-GlcNAcylation has recently received remarkable attention as 'an intracellular nutrient sensor' that can regulate diverse cellular processes in response to nutritional status [8].

O-GlcNAcylation is conserved throughout species. *O*-GlcNAc modification in *Caenorhabditis elegans* plays an important role in longevity, stress and immunity [9]. In drosophila, knockdown of *Ogt* reduced IGF homologue expression, thereby affecting organism growth and glucose metabolism [10]. These observations indicate a potential role for *O*-GlcNAcylation in glucose metabolism in mammals. Indeed, previous studies in cultured cells have demonstrated that *O*-GlcNAcylation is involved in glucose metabolism in the liver [11], skeletal muscle [12] and adipose tissues [13], and accelerates insulin secretion in pancreatic beta cells [14]. However, little is known about the physiological roles of this post-translational modification in glucose metabolism in vivo because congenital *Ogt*-knockout (KO) mice are embryonic lethal [15].

In this study, to reveal the physiological role of *O*-GlcNAcylation in glucose metabolism in living mice, tamoxifen (TM)-inducible global *Ogt*-KO mice were analysed. In addition, mice lacking *Ogt* in glucose metabolism-related tissues, including the liver, skeletal muscle, adipose tissues and pancreatic beta cells, were analysed.

Methods

Animal experiments All animal handling and experimentation were conducted according to the guidelines of the Research Center for Animal Life Science at Shiga University of Medical Science. All experimental protocols were approved by the Gene Recombination Experiment Safety Committee and the Research Center for Animal Life Science at Shiga University of Medical Science. Global and tissue-specific *Ogt*-KO mice were generated using the Cre-LoxP system. *Ogt*-flox ($Ogt^{f/f}$) female mice [15] (Jackson Laboratory, Bar Harbor, ME, USA) were crossbred with *R26*-Cre-ER^{T2} [16] (Jackson Laboratory) to generate global *Ogt*-KO mice, and with *Alb*-Cre [17] (Jackson Laboratory), *Mlc1f*-Cre [18], *Adipoq*-Cre [19] and $Pdx1^{PB}$-CreER™ mice [20] to generate liver (*Ogt*-LKO), skeletal muscle (*Ogt*-MKO), adipose tissue (*Ogt*-FKO) and beta cell (*Ogt*-βKO) specific *Ogt*-KO mice, respectively. In *Ogt*-KO and *Ogt*-βKO mice, TM (Sigma Aldrich, St Louis, MO, USA) was injected i.p. for five consecutive days (0.15 g kg^{-1} day^{-1}) at approximately 10–12 weeks of age. Only male mice were used for all experiments. Except for this, all samples were included for further analysis.

Islet isolation study Primary mouse islets from *Ogt*-flox and *Ogt*-βKO mice were isolated by collagenase digestion as described previously with slight modifications [21].

Blood analysis Blood glucose concentrations were measured with GDH-PQQ glucose test strips (Glutest Sensor, Sanwa Kagaku, Nagoya, Japan). Plasma insulin and glucagon levels were measured by ELISA (Morinaga, Tokyo, Japan, and Mercodia, Uppsala, Sweden).

Insulin and glucose tolerance tests Mice were i.p. injected with 0.5 U/kg insulin or 1 g/kg glucose after fasting for 6–8 h. Blood glucose levels were determined 15, 30, 60, 90 and 120 min after injection.

Histological analyses Fixed specimens embedded in paraffin were sectioned (3 μm thickness). Antibodies to O-linked *N*-acetylglucosamine (1:200, ab2739, Abcam, Cambridge, UK), insulin (1:500, ab7842, Abcam) and Ki67 (1:100, ab16667, Abcam) were used. Transmission electron microscopic analysis was performed with the Hitachi H-7500 (Hitachi, Tokyo, Japan). Cell apoptosis was analysed using the TACS2 TdT In Situ Apoptosis Detection Kit (Trevigen, Gaithersburg, MD, USA).

Total RNA preparation and qRT-PCR analysis Total RNA was extracted from tissues using the RNeasy Kit (Qiagen, Valencia, CA, USA). cDNA was synthesised using reverse transcription reagents (Takara Bio, Otsu, Japan). Transcript abundance was assessed by real-time PCR on an Applied Biosystems 7500 Real-Time PCR System (PerkinElmer Applied Biosystems, Foster City, CA, USA) with SYBR Green (Bio-Rad Laboratories, Hercules, CA, USA). Analytical data were

adjusted with *36B4* mRNA expression as an internal control. Primer sequences are provided in the electronic supplementary material (ESM) Table 1.

Western blot analysis For western blot analysis, proteins were resolved by SDS-PAGE and transferred to nitrocellulose membranes. The membranes were then incubated with the following antibodies: OGT (1:1000, O6264, Sigma Aldrich); MGEA5 (3:10,000, ab124807, Abcam); RL2 (1:1000, MA1-072, Thermo Scientific, MA, USA); Actin (1:10,000, sc-1616, Santa Cruz Biotechnology, CA, USA) and β Actin (1:10,000, A5316, Sigma Aldrich). After additional washing, the membranes were incubated with horseradish peroxidase-linked secondary antibodies before chemiluminescence detection.

Statistical analysis Data are expressed as means ± SEM. MANOVA followed by the Student's *t* test was used for time course analysis. Student's *t* tests were used to assess differences between two groups. The logrank test was performed for survival curves. A p value <0.05 was considered to be statistically significant.

Results

***Ogt* deletion in adult mice resulted in a lethal phenotype accompanied by body weight loss and hypoglycaemia** We first clarified the physiological role of *O*-GlcNAcylation in glucose metabolism in adult mice. Congenital global *Ogt* deletion is embryonic lethal, indicating that *Ogt* is critical for development in mice [15]. TM-inducible global *Ogt*-KO mice were generated by crossbreeding *Ogt*-flox female mice [15] with *R26*-Cre-ER^{T2} male mice [16] (Fig. 1a). At 10 weeks of age, *Ogt* deletion was induced by i.p. TM injection (Fig. 1a). Immunohistochemical analysis demonstrated that *O*-GlcNAcylation was present in both the nucleus and cytosol of liver, skeletal muscle, adipose tissue cells and particularly pancreatic islets, and *O*-GlcNAcylation was absent from these tissues in *Ogt*-KO mice (Fig. 1b). In addition, western blot analysis revealed decreases in Ogt and *O*-GlcNAcylation (RL2) levels in other tissues with varying magnitudes (ESM Fig. 1a). Following TM injection, *Ogt*-KO mice gradually lost weight accompanied by loss of body fat mass (Fig. 1c, d). Moreover, blood glucose and plasma insulin levels also gradually decreased (Fig. 1e, f). At 4 weeks after TM injection, *Ogt*-KO mice exhibited hypothermia and severe malnutrition, although their food intake did not significantly decrease (Fig. 1g, h, ESM Table 2). Finally, *Ogt*-KO mice began to die, and only 20% of *Ogt*-KO mice survived until 6 weeks after TM injection (Fig. 1i). As a result, we were unable to analyse glucose metabolism in these mice. These data indicate that *O*-GlcNAcylation is essential not only for embryonic development but also for survival in adult mice.

To examine the role of *O*-GlcNAcylation in glucose metabolism, we generated tissue-specific *Ogt*-KO mice and analysed the role of *O*-GlcNAcylation in each tissue.

Insulin-sensitive tissue-specific *Ogt* deletion had no major effects on glucose metabolism We generated tissue-specific *Ogt*-KO mice for insulin-sensitive tissues, including liver (*Ogt*-LKO), skeletal muscle (*Ogt*-MKO) and adipose tissue (*Ogt*-FKO), by crossbreeding *Ogt*-flox mice with *Alb*-Cre [17], *Mlc1f*-Cre [18] and *Adipoq*-Cre mice [19], respectively (ESM Fig. 2a). Western blot analysis indicated significant decreases in OGT protein levels and *O*-GlcNAcylation in these tissues (ESM Fig. 2b, c). *Ogt*-LKO, *Ogt*-MKO and *Ogt*-FKO mice grew normally and displayed no significant changes in fasting glucose levels compared with those of control littermates at 10 weeks of age (Fig. 2a–f). Furthermore, insulin-sensitive tissue-specific *Ogt*-KO mice exhibited normal glucose levels during an IPGTT. Additionally, they displayed little difference in insulin sensitivity by insulin tolerance test compared with control littermates (Fig. 2g–l). Since *Ogt* knockdown in insulin-sensitive tissues had little impact on glucose metabolism under physiological conditions, we evaluated the role of *O*-GlcNAcylation in pancreatic beta cells.

Pancreatic beta cell-specific *Ogt*-KO mice displayed biphasic changes in glucose metabolism To evaluate the role of *Ogt* in glucose metabolism in pancreatic beta cells, we generated TM-inducible beta cell-specific *Ogt*-KO mice (*Ogt*-βKO) by crossbreeding female *Ogt*-flox mice with male *Pdx1*-CreER™ mice [20] (Fig. 3a). At 10 weeks of age, TM was injected i.p. in both groups of mice. Western blot and immunohistochemical analyses indicated that OGT protein levels and protein *O*-GlcNAcylation were markedly diminished in pancreatic beta cells from *Ogt*-βKO mice (Fig. 3b–e). Interestingly, in *Ogt*-βKO mice body weight was markedly increased 6 weeks after TM injection because of mild hyperphagia but subsequently decreased from 8 weeks post-injection (Fig. 3f, ESM Fig. 3a). In contrast, *Ogt*-βKO blood glucose levels transiently decreased at 5–6 weeks and then dramatically increased after 8 weeks post-injection (Fig. 3g). Finally, *Ogt*-βKO mice displayed severe hyperglycaemia at 10 weeks post-injection (Fig. 3g). Consistent with temporal changes in glucose levels, plasma insulin levels in *Ogt*-βKO mice transiently increased 5–7 weeks post-injection and were eventually depleted at 10 weeks (Fig. 3h). IPGTT were performed every week between 5 and 8 weeks post-injection. The results indicated a biphasic change in glucose tolerance, with a hypoglycaemic state occurring at 5–6 weeks post-injection (early phase) and a hyperglycaemic state occurring at 7–8 weeks post-injection (late phase) (Fig. 3i–m).

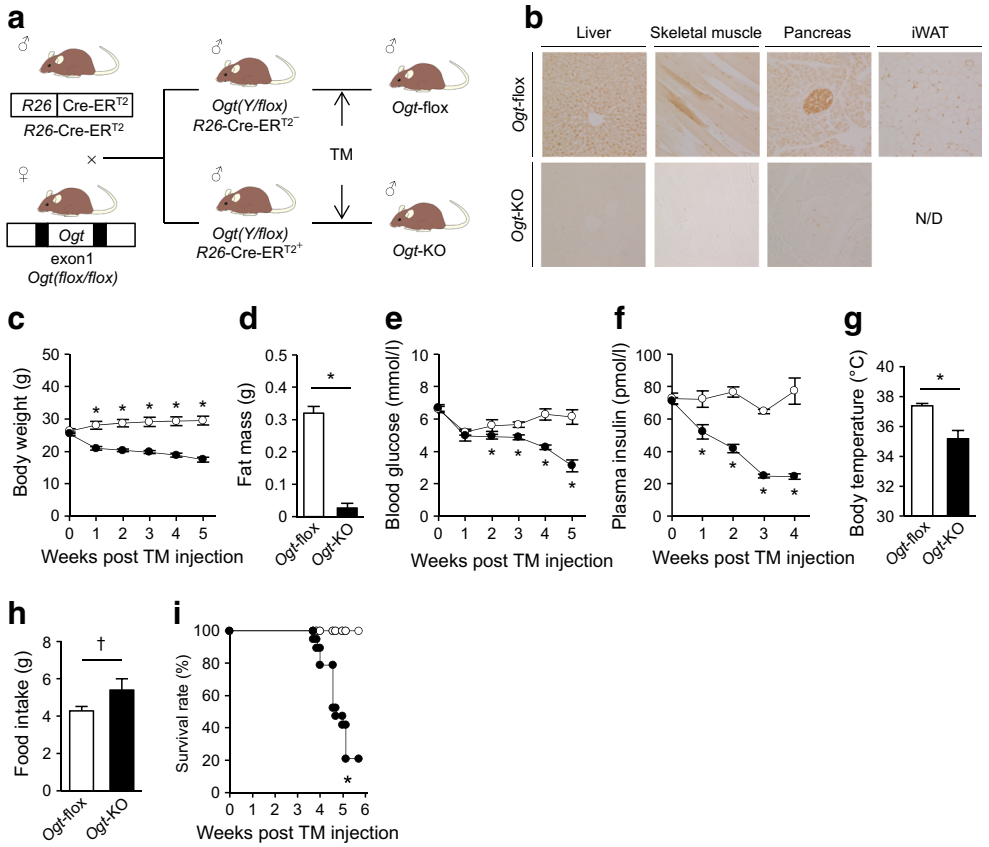

Fig. 1 Inducible *Ogt* deletion in adult mice resulted in a lethal phenotype. (**a**) Schematic diagram of *Ogt*-KO mouse generation. (**b**) Immunohistochemical analysis of *O*-GlcNAcylation using anti-*O*-GlcNAc (RL2) antibodies in multiple tissues (original magnification ×100). iWAT, inguinal white adipose tissue; N/D, not determined due to lean phenotype. (**c**) Body weight of *Ogt*-KO mice and control mice following TM injection (n = 6 for *Ogt*-flox and n = 10 for *Ogt*-KO). (**d**) Inguinal fat mass of *Ogt*-KO mice and control mice 3 weeks after TM injection (n = 3 each). (**e**) Blood glucose levels of *Ogt*-KO mice and control mice following TM injection (n = 6 for *Ogt*-flox and n = 10 for *Ogt*-KO). (**f**) Plasma insulin levels of *Ogt*-KO mice and control mice following TM injection (n = 6 for *Ogt*-flox and n = 10 for *Ogt*-KO). (**g**) Body temperature of *Ogt*-KO mice and control mice 3 weeks after TM injection (n = 5 for *Ogt*-flox and n = 4 for *Ogt*-KO). (**h**) Food intake of *Ogt*-KO mice and control mice 3 weeks after TM injection (n = 8 for *Ogt*-flox and n = 6 for *Ogt*-KO). (**i**) Survival rates following TM injection (n = 8 for *Ogt*-flox and n = 18 for *Ogt*-KO). White circles, *Ogt*-flox; black circles, *Ogt*-KO. In (**c**), (**e**) and (**f**) MANOVA Pillai's trace $p < 0.01$, $p < 0.05$, $p < 0.05$, respectively. Data are means ± SEM. $^{*}p < 0.05$, $^{\dagger}p = 0.08$

Transient hyperinsulinaemia improved glucose tolerance and accelerated adiposity during the early phase *Ogt*-βKO mice displayed lower glucose levels during the early phase but hyperglycaemia during the late phase (Fig. 3g). During the early phase, we observed significant increases in body weight in *Ogt*-βKO mice (Figs 3f, 4a). Furthermore, marked steatosis and increased adiposity in *Ogt*-βKO mice could be explained by hyperphagia resulting from enhanced insulin secretion followed by hypoglycaemia (Fig. 4b, c). In fact, *Ogt*-βKO mice displayed increased insulin secretion in response to a glucose challenge prior to weight gain (Fig. 4d, e). Histological analysis demonstrated that islet area, size and Ki67 positive cells were increased in *Ogt*-βKO mice (Fig. 4f–i), but no significant changes were detected in pancreatic islets by immunohistochemistry for insulin (Fig. 4j, k). Moreover, insulin secretion and content per isolated islet was increased in *Ogt*-βKO mice (Fig. 4l, m) and was accompanied by increased expression of the gene encoding insulin (*Ins2*) (Fig. 4n). These findings suggest that loss of *O*-GlcNAcylation in pancreatic beta cells may have lowered glucose levels during the early phase by increasing insulin secretion and enhancing islet growth. Taken together, in the early phase, deletion of *Ogt*-mediated *O*-GlcNAcylation resulted in accelerated insulin secretion in vivo, accompanied by increased insulin expression and islet growth, resulting in enhanced insulin-induced adiposity in vivo.

Depletion of *Ogt* resulted in hypoinsulinaemia because of beta cell apoptosis During the late phase, a significant increase in blood glucose levels was accompanied by depleted insulin secretion (Figs 3g, h, 5a, b). Histological analysis demonstrated decreased islet number and size (Fig. 5c–e). Furthermore, insulin-positive area was significantly decreased in *Ogt*-βKO mice compared with control mice (Fig. 5f, g). Transmission electron microscopic analysis revealed fewer insulin granules with abnormal morphology (Fig. 5h).

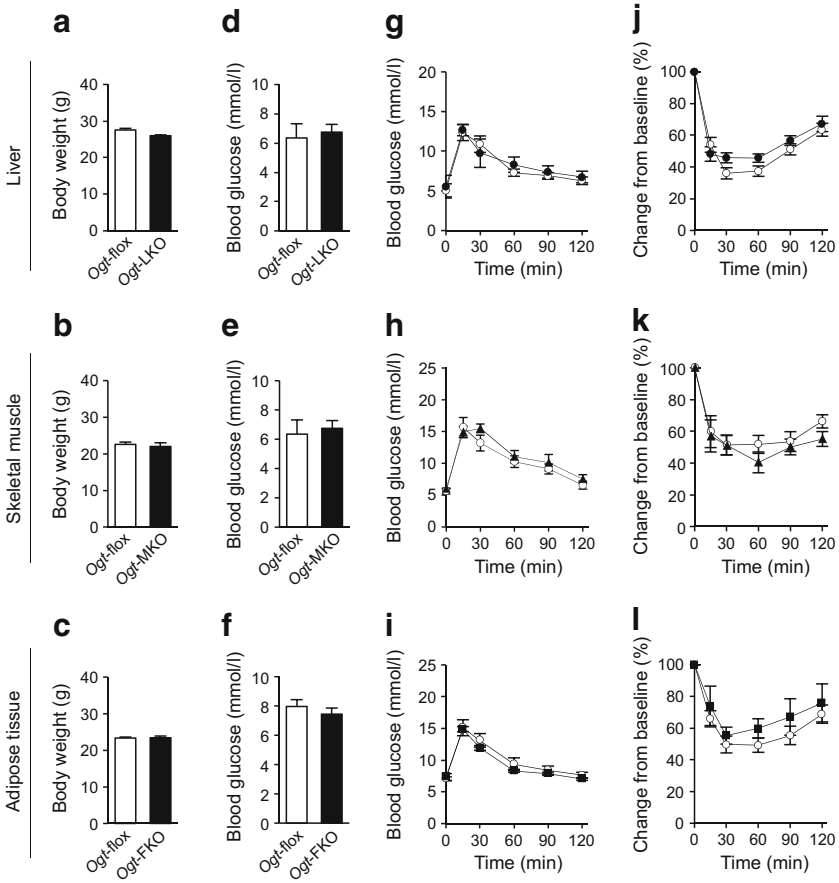

Fig. 2 *Ogt* deletion in insulin-sensitive tissues had little impact on glucose metabolism. (**a**–**c**) Body weights and (**d**–**f**) blood glucose levels of insulin-sensitive tissue-specific *Ogt*-KO mice and littermate control mice at 10 weeks of age (n = 5–6 each). (**g**–**i**) Blood glucose concentrations during IPGTT (n = 4–5 each). MANOVA Pillai's trace p = 0.964, p = 0.191, p = 0.926, respectively. (**j**–**l**) Glucose changes from baseline during i.p. insulin tolerance tests (n = 4–9 each). MANOVA Pillai's trace p = 0.182, p = 0.879, p = 0.525, respectively. White circles, *Ogt*-flox; black circles, *Ogt*-LKO; black triangles, *Ogt*-MKO; black squares, *Ogt*-FKO. Data are means ± SEM

Similarly, insulin and beta cell-related gene expression levels were significantly reduced (Fig. 5i). TUNEL staining indicated a significant increase in apoptotic cells in *Ogt*-βKO mouse islets (Fig. 5j, k). These findings suggest that *Ogt*-mediated *O*-GlcNAcylation is essential for beta cell survival.

Discussion

In this study, we comprehensively evaluated the role of *O*-GlcNAcylation in glucose metabolism in multiple tissues using tissue-specific *Ogt*-KO mice under physiological conditions. Because congenital *Ogt* gene deletion in mice caused embryonic lethality [15], little was known about the role of *O*-GlcNAcylation in systemic glucose metabolism. In this study, for the first time, we generated TM-inducible systemic *Ogt*-KO mice, which allowed us to analyse the role of *O*-GlcNAcylation in glucose metabolism in adult mammals. *Ogt*-KO mice displayed gradual body weight loss (Fig. 1c). Furthermore, *Ogt*-KO mouse mortality rates increased dramatically 4 weeks after TM injection (Fig. 1i). These results suggest that *O*-GlcNAcylation is essential not only for organ development in embryos but also for survival in adult mice.

Next we created insulin-sensitive tissue-specific *Ogt*-KO mice. *Ogt* knockdown in liver, skeletal muscle and adipose tissue had minimal impact on glucose homeostasis under physiological conditions (Fig. 2). In contrast to our results, previous studies have reported that excess *O*-GlcNAcylation in mice led to insulin resistance [22–24]. Collectively, these results suggest that gain-of-function of *O*-GlcNAcylation in insulin-sensitive organs is associated with the pathogenesis of insulin resistance, whereas loss-of-function does not impact glucose metabolism under physiological conditions. Further examination is necessary to investigate the loss of *O*-GlcNAcylation during various pathological conditions (e.g. diabetes), starvation and exercise.

A prominent phenotype was observed in *Ogt*-βKO mice. Acquired *Ogt* deletion revealed a unique phenotype. Specifically, mice displayed reduced glucose levels accompanied by enhanced insulin secretion during the early phase and hyperglycaemia accompanied by insulin depletion during the late phase (Fig. 3h–k). A recent study reported that loss of *Ogt* in pancreatic beta cells induced severe hyperglycaemia and insulin depletion, potentially because of endoplasmic reticulum (ER) stress, using a similar mouse model [25]. Their results were consistent with the late phase phenotype of our study, and increased levels of ER stress markers, such as *Chop*

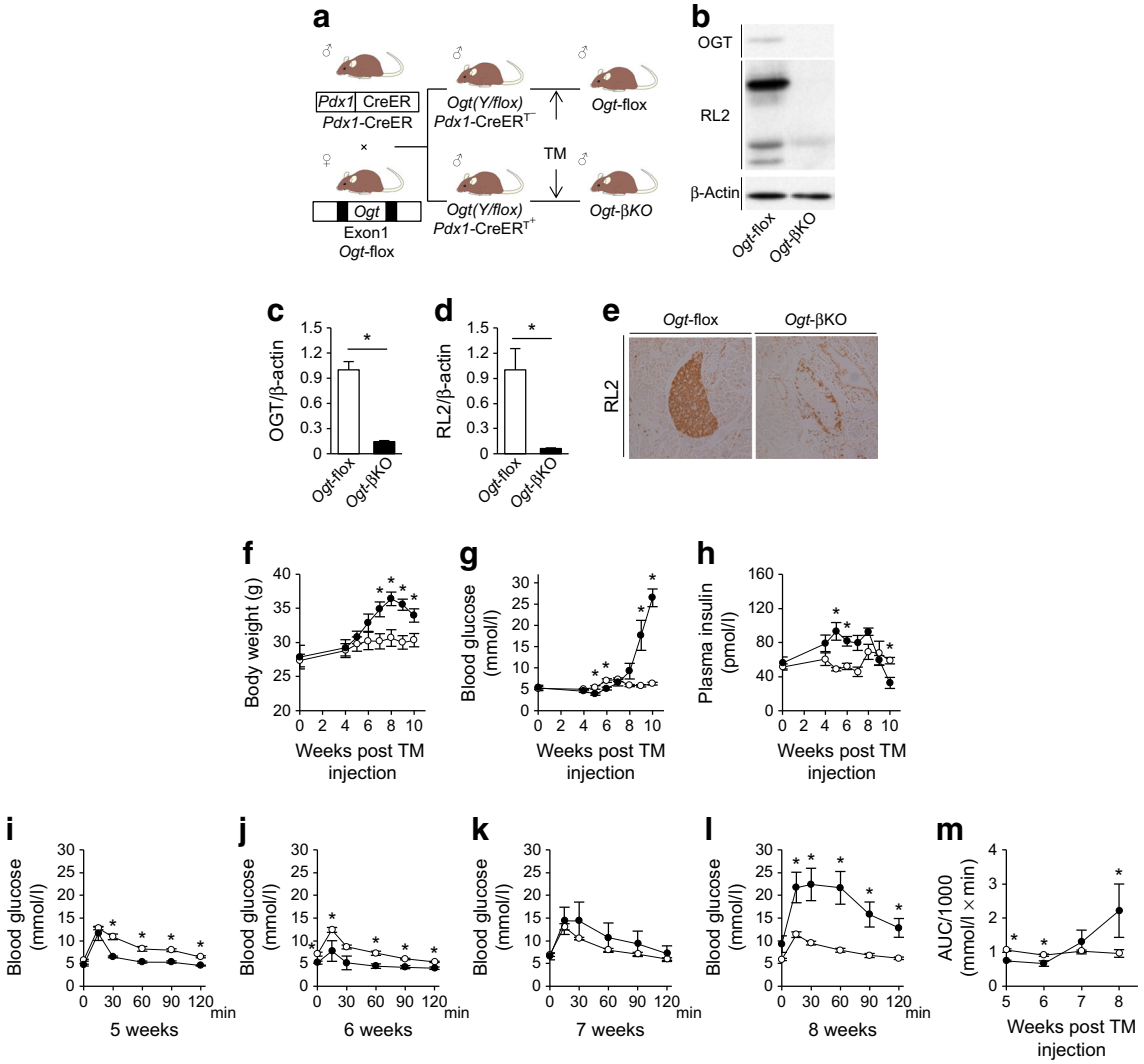

Fig. 3 *Ogt* deletion in pancreatic beta cells resulted in biphasic changes in body weight and glucose metabolism. (**a**) Schematic diagram of pancreatic beta cell-specific *Ogt*-βKO mouse generation. (**b**) Representative western blot analysis for OGT and *O*-GlcNAcylation (RL2) levels in isolated islets. (**c**, **d**) Quantification of western blot analysis for OGT and RL2 ($n = 4$ each). (**e**) Representative immunohistochemical analysis for RL2 in the pancreas of *Ogt*-βKO and control mice at 4 weeks post-TM injection (original magnification ×100). (**f**–**h**) Temporal changes in body weight and blood glucose and plasma insulin levels in *Ogt*-βKO mice and control mice following TM injection ($n = 7$ for *Ogt*-flox and $n = 8$ for *Ogt*-βKO). (**i**–**l**) Glucose concentrations during IPGTT 5–8 weeks, respectively, after TM injection ($n = 7$ for *Ogt*-flox and $n = 8$ for *Ogt*-βKO). (**m**) Gradual changes in AUC during IPGTT 5–8 weeks after TM injection ($n = 7$ for *Ogt*-flox and $n = 8$ for *Ogt*-βKO). MANOVA Pillai's trace: (**f**, **h**) $p < 0.05$; (**g**, **i**, **j**, **l**, **m**) $p < 0.01$; (**k**) $p = 0.592$. White circles, *Ogt*-flox; black circles, *Ogt*-βKO. Data are means ± SEM. $^*p < 0.05$

and *Bip*, were also observed in our model. Additionally, our study revealed that *Ogt* deletion transiently promoted insulin secretion and beta cell growth and subsequently increased adiposity during the early phase (Fig. 3). These results suggest that *O*-GlcNAcylation regulates not only beta cell survival but also insulin secretion and beta cell capacity under physiological conditions.

Two unresolved issues remain. The first issue is a technical limitation. A recent study reported that *Pdx1*^{PB}-CreER™ mice also express Cre in pancreatic alpha cells and the hypothalamus [26]. In our model, there were no significant differences in plasma glucagon levels between *Ogt*-βKO mice and control littermates, suggesting a limited effect of *Ogt* deletion on glucagon secretion (ESM Fig. 3b). In the hypothalamus, a recent report demonstrated that loss of *O*-GlcNAcylation in paraventricular nucleus neurons resulted in a rapid obese phenotype in which food intake more than doubled within 2 weeks following Cre induction [27]. Our mouse model also displayed transient obesity with mild hyperphagia. However, the increase in food intake was modest, and body weight gain was delayed compared with mice lacking *O*-GlcNAcylation in paraventricular nucleus neurons (ESM Fig. 3a). Furthermore, we observed hyperinsulinaemia and hypoglycaemia in the mice 5–6 weeks after *Ogt* deletion. Hypoglycaemia induced

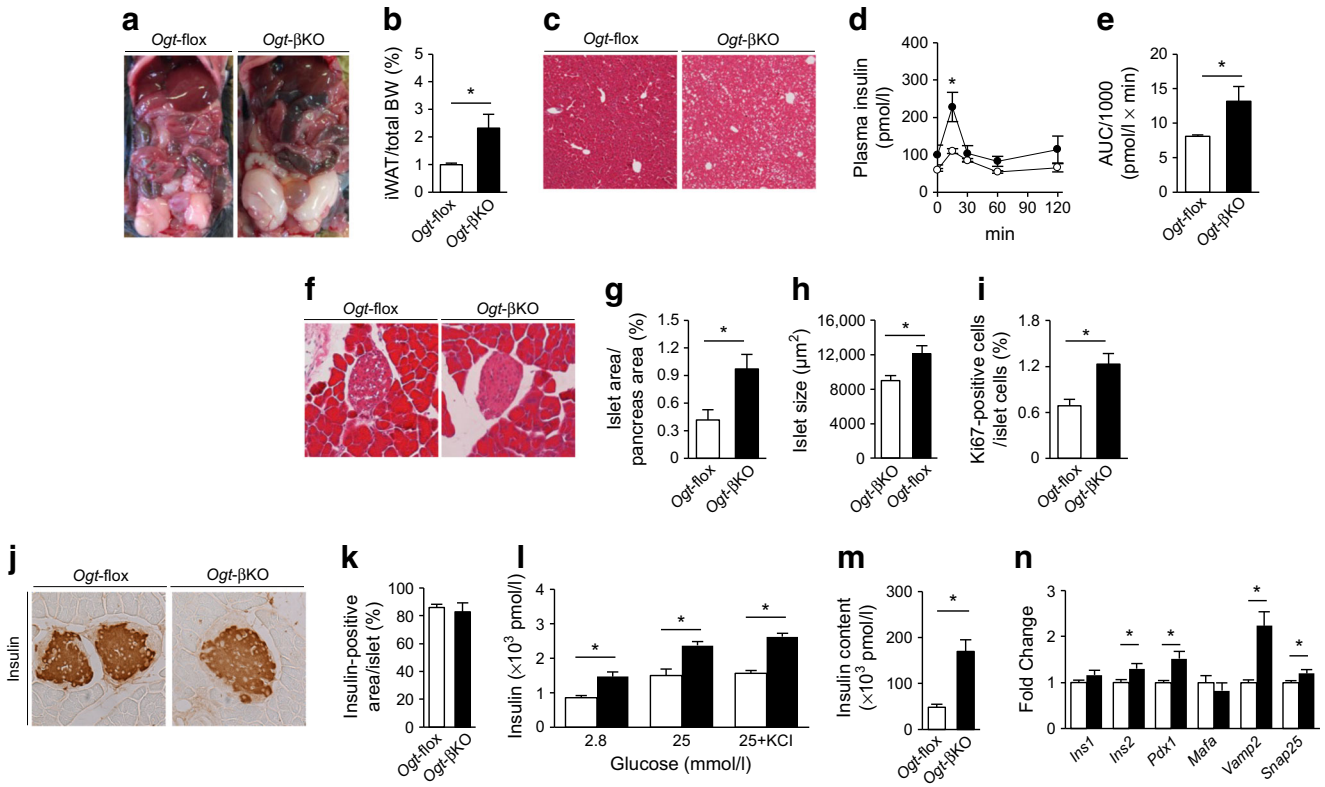

Fig. 4 Loss of *O*-GlcNAcylation in pancreatic beta cells resulted in transient hyperinsulinaemia and subsequent adiposity. (**a**) Representative images of a beta cell-specific *Ogt*-βKO mouse and a control mouse 7 weeks after TM injection. (**b**) iWAT mass of *Ogt*-βKO and control mice ($n = 6$ each). BW, body weight. (**c**) Liver H&E staining of *Ogt*-βKO and control mice (original magnification ×100). (**d**, **e**) Insulin secretion and AUC during IPGTT in *Ogt*-βKO and control mice 5 weeks after TM injection ($n = 7$ for *Ogt*-flox and $n = 8$ for *Ogt*-βKO). In (**d**), MANOVA Pillai's trace $p < 0.05$. (**f**–**h**) Representative H&E staining, islet/pancreas area and islet size in *Ogt*-βKO and control mice 5 weeks after TM injection (original magnification ×100). (**i**) Ki67 positive cells/islets in *Ogt*-βKO and control mice 5 weeks after TM injection. (**j**, **k**) Representative insulin immunohistochemical images and quantification ($n = 6$ each; original magnification ×100). (**l**) Insulin secretion in response to 2.8 mmol/l glucose, 25 mmol/l glucose and 25 mmol/l glucose +30 mmol/l KCl from isolated islets (ten islets; $n = 4$–5 each). (**m**) Insulin content in isolated islets from *Ogt*-βKO and control mice (ten islets; $n = 12$ for *Ogt*-flox and $n = 15$ for *Ogt*-βKO). (**n**) qPCR analysis of isolated islets from *Ogt*-βKO and control mice ($n = 5$ each). White circles and bars, *Ogt*-flox; black circles and bars, *Ogt*-βKO. Data are means ± SEM. *$p < 0.05$

by hyperinsulinaemia is often accompanied by hyperphagia to alleviate hypoglycaemia. Therefore, it induces weight gain, which is often observed in people with type 2 diabetes receiving insulin treatment [28, 29]. Thus, we speculate that body weight gain between 5 and 8 weeks post-deletion is a secondary effect resulting from hypoglycaemia rather than an effect in the hypothalamus. Further investigation will be necessary to confirm the direct effects in pancreatic beta cells.

Second, the cause of death in the global *Ogt*-KO mouse is unclear. Although *Ogt*-βKO mice exhibited severe hyperglycaemia, none of the tissue-specific KO mice displayed the mortality rates observed in the global *Ogt*-KO mouse. One recent study demonstrated that heart-specific *Ogt* deletion was also lethal because of heart failure [30]. However, we did not detect elevated *Bnp* (also known as *Nppb*) mRNA expression in *Ogt*-KO mice (ESM Fig. 1b). Interestingly, although food intake did not decrease, severe malnutrition and hypometabolism were observed before death (ESM Table 2). Thus, we speculate that heart failure was not responsible for increased mortality rates in this model; however, malabsorption of nutrients could be the cause of the increased mortality rates. In addition, our results from global and beta cell-specific *Ogt*-KO mice clearly indicate that *O*-GlcNAcylation inhibition is inappropriate for the treatment of insulin resistance and diabetes complications because of its harmful effects. A recent proteomics approach revealed over 1000 OGT targets in mammalian cells [31]. Identification of the specific *O*-GlcNAcylated protein may provide a novel therapeutic strategy for the treatment of diabetes mellitus.

In conclusion, *O*-GlcNAcylation plays a pivotal role in glucose and cellular homeostasis in adult mammals. In addition, *O*-GlcNAcylation in insulin-sensitive tissues does not substantially impact glucose metabolism under physiological conditions, whereas *O*-GlcNAcylation in pancreatic beta cells has multiple effects on insulin secretion and beta cell homeostasis.

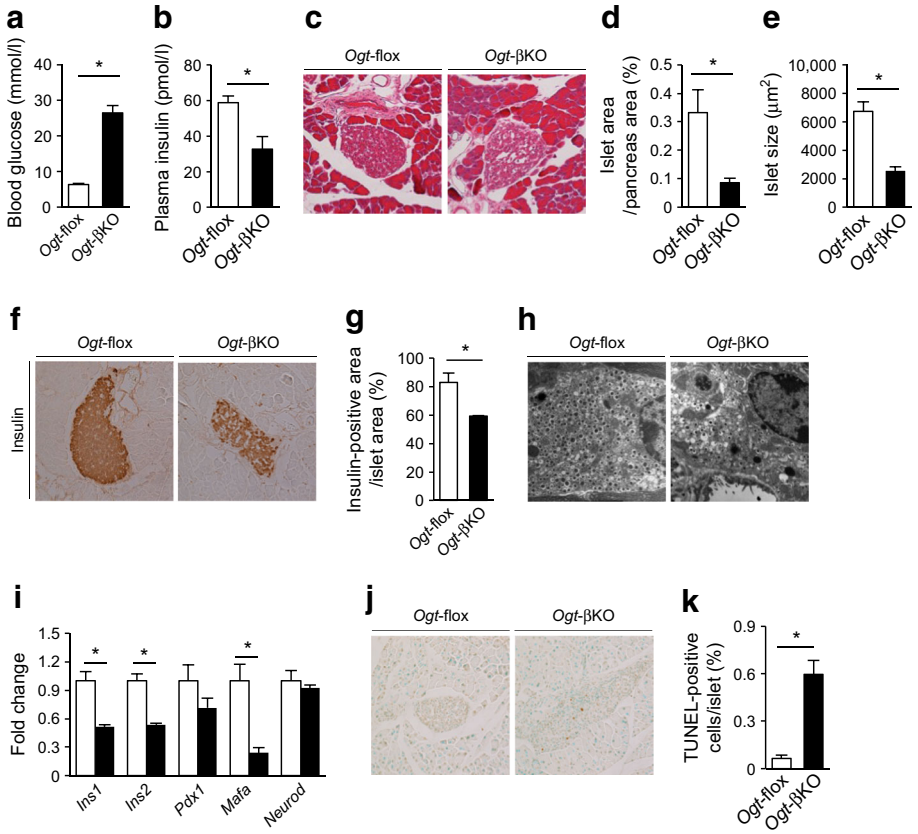

Fig. 5 *Ogt*-βKO mice displayed severe hyperglycaemia and insulin depletion associated with beta cell apoptosis. (**a**, **b**) Blood glucose and plasma insulin levels in *Ogt*-βKO and control mice 10 weeks after TM injection (n = 7 for *Ogt*-flox and n = 5 for *Ogt*-βKO). (**c**–**e**) Representative H&E staining, islet/pancreas area and islet size in *Ogt*-βKO and control mice 10 weeks after TM injection (original magnification ×100). (**f**, **g**) Insulin immunohistochemistry and quantification of insulin-positive area/islet (n = 6 each; original magnification ×100). (**h**) Transmission electron microscopy of *Ogt*-βKO and control mice 10 weeks after TM injection (original magnification ×2000). (**i**) qPCR analysis of isolated islets (n = 5 each). (**j**, **k**) TUNEL staining and TUNEL-positive cells/islet (n = 6 each; original magnification ×100). White bars, *Ogt*-flox; black bars, *Ogt*-βKO. Data are means ± SEM. *$p < 0.05$

Acknowledgements We are indebted to K. Kosaka, Y. Asano, T. Yamamoto and the Central Research Laboratory of Shiga University of Medical Science for their expert technical assistance in this study. We thank S.J. Burden (New York University Medical Center) and K. Ueki (Tokyo University) for providing *Mlc1f*-Cre mice. We also thank E. Rosen (Harvard University), W. Ogawa and T. Hosooka (Kobe University) for providing *Adipoq*-Cre mice, and M. Gannon (Vanderbilt University Medical Center) for providing *Pdx1*^{PB}-CreER™ mice. Some of the data were presented as abstracts at the 75th Scientific Sessions of the ADA in 2015 and Keystone Symposia in 2015, and have been submitted to the third Korea–Japan Diabetes Forum in 2017.

Data availability The data that support the findings of this study are available from the corresponding author upon reasonable request.

Funding This study was supported by Grants-in-Aid for Scientific Research (KAKENHI) from the Japan Society for the Promotion of Science (No. 15K09383 to OS, No. 16K09743 to SU, No. 16K09744 to KM). This study was partially supported by the Shiga University of Medical Science President's Grant for the Encouragement of Young Researchers. The study was funded by the Shiga University of Medical Science. The Department of Medicine, Shiga University of Medical Science reports receiving research promotion grants (Shogaku Kifukin) from Astellas, Boehringer-Ingelheim, Daiichi-Sankyo, Kowa Pharmaceuticals, Kyowa Hakko Kirin, Mitsubishi Tanabe, MSD, Ono Pharmaceutical, Sanofi, Sanwa Kagaku Kenkyusho, Shionogi, Taisho-Toyama, Takeda and Teijin Pharma. However, the research topics of these donation grants are not restricted.

Duality of interest The authors declare that there is no duality of interest associated with this manuscript.

Contribution statement SI, OS, SK, SU and HM designed the study. SI, OS, NO, KI and NH conducted the research. SI, KM, TC, NH and NI analysed and interpreted the data. SI, KM and HM wrote the manuscript. OS, NO, KM, SU, SK, TC, KI, NH, NI and HM reviewed and edited the manuscript. KM had primary responsibility for the final content. All authors read and approved the final manuscript.

References

1. Kahn BB, Alquier T, Carling D, Hardie DG (2005) AMP-activated protein kinase: ancient energy gauge provides clues to modern understanding of metabolism. Cell Metab 1:15–25

2. Popovic D, Vucic D, Dikic I (2014) Ubiquitination in disease pathogenesis and treatment. Nat Med 20:1242–1253
3. Menzies KJ, Zhang H, Katsyuba E, Auwerx J (2016) Protein acetylation in metabolism—metabolites and cofactors. Nat Rev Endocrinol 12:43–60
4. Hanover JA, Krause MW, Love DC (2012) Bittersweet memories: linking metabolism to epigenetics through O-GlcNAcylation. Nat Rev Mol Cell Biol 13:312–321
5. Hardiville S, Hart GW (2014) Nutrient regulation of signaling, transcription, and cell physiology by *O*-GlcNAcylation. Cell Metab 20:208–213
6. Torres CR, Hart GW (1984) Topography and polypeptide distribution of terminal *N*-acetylglucosamine residues on the surfaces of intact lymphocytes. Evidence for O-linked GlcNAc. J Biol Chem 259:3308–3317
7. Janetzko J, Walker S (2014) The making of a sweet modification: structure and function of *O*-GlcNAc transferase. J Biol Chem 289: 34424–34432
8. Zachara NE, Hart GW (2004) O-GlcNAc a sensor of cellular state: the role of nucleocytoplasmic glycosylation in modulating cellular function in response to nutrition and stress. Biochim Biophys Acta 1673:13–28
9. Love DC, Ghosh S, Mondoux MA et al (2010) Dynamic *O*-GlcNAc cycling at promoters of *Caenorhabditis elegans* genes regulating longevity, stress, and immunity. Proc Natl Acad Sci USA 107:7413–7418
10. Sekine O, Love DC, Rubenstein DS, Hanover JA (2010) Blocking O-linked GlcNAc cycling in drosophila insulin-producing cells perturbs glucose-insulin homeostasis. J Biol Chem 285:38684–38691
11. Ruan HB, Han X, Li MD et al (2012) *O*-GlcNAc transferase/host cell factor C1 complex regulates gluconeogenesis by modulating PGC-1alpha stability. Cell Metab 16:226–237
12. Wang X, Feng Z, Wang X et al (2016) *O*-GlcNAcase deficiency suppresses skeletal myogenesis and insulin sensitivity in mice through the modulation of mitochondrial homeostasis. Diabetologia 59:1287–1296
13. Vosseller K, Wells L, Lane MD, Hart GW (2002) Elevated nucleocytoplasmic glycosylation by *O*-GlcNAc results in insulin resistance associated with defects in *Akt* activation in 3T3-L1 adipocytes. Proc Natl Acad Sci USA 99:5313–5318
14. Gao Y, Miyazaki J, Hart GW (2003) The transcription factor PDX-1 is post-translationally modified by O-linked *N*-acetylglucosamine and this modification is correlated with its DNA binding activity and insulin secretion in min6 beta cells. Arch Biochem Biophys 415:155–163
15. Shafi R, Iyer SP, Ellies LG et al (2000) The *O*-GlcNAc transferase gene resides on the X chromosome and is essential for embryonic stem cell viability and mouse ontogeny. Proc Natl Acad Sci USA 97:5735–5739
16. Ventura A, Kirsch DG, McLaughlin ME et al (2007) Restoration of p53 function leads to tumour regression in vivo. Nature 445:661–665
17. Weisend CM, Kundert JA, Suvorova ES, Prigge JR, Schmidt EE (2009) Cre activity in fetal *alb*Cre mouse hepatocytes: utility for developmental studies. Genesis 47:789–792
18. Bothe GW, Haspel JA, Smith CL, Wiener HH, Burden SJ (2000) Selective expression of Cre recombinase in skeletal muscle fibers. Genesis 26:165–166
19. Eguchi J, Wang X, Yu S et al (2011) Transcriptional control of adipose lipid handling by IRF4. Cell Metab 13:249–259
20. Zhang H, Fujitani Y, Wright CV, Gannon M (2005) Efficient recombination in pancreatic islets by a tamoxifen-inducible Cre-recombinase. Genesis 42:210–217
21. Fujimoto S, Ishida H, Kato S et al (1998) The novel insulinotropic mechanism of pimobendan: direct enhancement of the exocytotic process of insulin secretory granules by increased Ca2+ sensitivity in beta cells. Endocrinology 139:1133–1140
22. Virkamaki A, Daniels MC, Hamalainen S, Utriainen T, McClain D, Yki-Jarvinen H (1997) Activation of the hexosamine pathway by glucosamine in vivo induces insulin resistance in multiple insulin sensitive tissues. Endocrinology 138:2501–2507
23. McClain DA, Lubas WA, Cooksey RC et al (2002) Altered glycan-dependent signaling induces insulin resistance and hyperleptinemia. Proc Natl Acad Sci U S A 99:10695–10699
24. Yang X, Ongusaha PP, Miles PD et al (2008) Phosphoinositide signalling links *O*-GlcNAc transferase to insulin resistance. Nature 451:964–969
25. Alejandro EU, Bozadjieva N, Kumusoglu D et al (2015) Disruption of O-linked *N*-acetylglucosamine signaling induces ER stress and beta cell failure. Cell Rep 13:2527–2538
26. Wicksteed B, Brissova M, Yan W et al (2010) Conditional gene targeting in mouse pancreatic β-cells: analysis of ectopic Cre transgene expression in the brain. Diabetes 59:3090–3098
27. Lagerlof O, Slocomb JE, Hong I et al (2016) The nutrient sensor OGT in PVN neurons regulates feeding. Science 351:1293–1296
28. The Diabetes Control and Complications Trial Research Group (1993) The effect of intensive treatment of diabetes on the development and progression of long-term complications in insulin-dependent diabetes mellitus. N Engl J Med 329:977–986
29. Dewan S, Gillett A, Mugarza JA, Dovey TM, Halford JC, Wilding JP (2004) Effects of insulin-induced hypoglycaemia on energy intake and food choice at a subsequent test meal. Diabetes Metab Res Rev 20:405–410
30. Watson LJ, Long BW, DeMartino AM et al (2014) Cardiomyocyte *Ogt* is essential for postnatal viability. Am J Physiol Heart Circ Physiol 306:H142–H153
31. Nagel AK, Ball LE (2014) *O*-GlcNAc transferase and *O*-GlcNAcase: achieving target substrate specificity. Amino Acids 46:2305–2316